J. Fluid Mech. (2010), *vol.* 659, *pp.* 116–126.
doi:10.1017/S0022112010003113

Assessment of direct numerical simulation data of turbulent boundary layers

PHILIPP SCHLATTER† AND RAMIS ÖRLÜ

Linné Flow Centre, KTH Mechanics, SE-100 44 Stockholm, Sweden

(Received 17 February 2010; revised 7 June 2010; accepted 7 June 2010;
first published online 16 July 2010)

Statistics obtained from seven different direct numerical simulations (DNSs) pertaining to a canonical turbulent boundary layer (TBL) under zero pressure gradient are compiled and compared. The considered data sets include a recent DNS of a TBL with the extended range of Reynolds numbers $Re_\theta = 500$–4300. Although all the simulations relate to the same physical flow case, the approaches differ in the applied numerical method, grid resolution and distribution, inflow generation method, boundary conditions and box dimensions. The resulting comparison shows surprisingly large differences not only in both basic integral quantities such as the friction coefficient c_f or the shape factor H_{12}, but also in their predictions of mean and fluctuation profiles far into the sublayer. It is thus shown that the numerical simulation of TBLs is, mainly due to the spatial development of the flow, very sensitive to, e.g. proper inflow condition, sufficient settling length and appropriate box dimensions. Thus, a DNS has to be considered as a numerical experiment and should be the subject of the same scrutiny as experimental data. However, if a DNS is set up with the necessary care, it can provide a faithful tool to predict even such notoriously difficult flow cases with great accuracy.

Key words: turbulent boundary layers, turbulence simulation

1. Introduction

More than hundred years have passed since the seminal lecture by Ludwig Prandtl in 1904, in which he introduced the boundary-layer concept. While considerable progress has been made over the last century, the simplest quantity, the mean streamwise velocity component, in the seemingly simplest flow cases, the fully developed turbulent channel and pipe flow as well as the zero-pressure-gradient (ZPG) turbulent boundary layer (TBL), is still far from being fully understood. The debate regarding the correct description of the overlap region, be it log or power law, the universality of the law of the wall or the von Kármán 'constant' for various flow cases as well as the skin-friction relation are a few of the prominent topics related to the streamwise mean velocity profile. Despite the advances in experimental set-ups and measurement techniques, the scatter as well as systematic differences between various mean velocity profiles is far beyond the accuracy needed in order to settle the ongoing debates. The trend in experiments over the last decade went towards higher Reynolds numbers (see e.g. Österlund 1999) in order to ensure a sufficient scale separation and a broader overlap region. The Reynolds number commonly used to describe boundary layers is

† Email address for correspondence: pschlatt@mech.kth.se

based on the momentum-loss thickness θ, the free-stream velocity U_∞ and viscosity ν, namely $Re_\theta = \theta U_\infty/\nu$.

While for channel flows, direct numerical simulations (DNSs) are competing with experiments in terms of the Reynolds number, the early simulations by Spalart (1988) at experimentally low Reynolds numbers ($Re_\theta = 300, 670$ and 1410) served for two decades as the standard reference case for ZPG TBL flows. Over the past years, a new interest in simulating spatially developing boundary layers with higher Re_θ has emerged, and today a number of simulation data are publicly available. While the quality of experiments has been scrutinized in detail (see e.g. in Fernholz & Finley 1996; Chauhan, Monkewitz & Nagib 2009), and the data have been utilized to test scaling laws to a level even beyond the experimental accuracy (e.g. Monkewitz, Chauhan & Nagib 2008) such an assessment has not yet been performed for corresponding DNS results. One particular reason might be due to the common trust in DNS, stemming from the very good agreement between simulations of channel flows, as well as the (rather marginal) qualitative 'validations' with experiments for the case of ZPG TBL simulations. Furthermore, some of the DNS data have already been utilized to test scaling laws (e.g. by Khujadze & Oberlack 2004; Buschmann, Indinger & Gad-el-Hak 2009) and are generally weighted stronger than experimental results in their respective Reynolds-number range.

Reviewing a large amount of literature data for (experimentally) low-Reynolds-number TBL measurements yields that most of these data are neither supplemented by direct and independent skin-friction measurement, nor do all of them adhere to accurately controlled ZPG equilibrium conditions (Örlü 2009). Consequently, there is a lack of fully established experimental reference data in the low-Re range. This observation directly prompts the need to critically assess the available DNS data for ZPG TBL flows, and motivates the current study. Here, the discussion is restricted to basic flow quantities such as integral parameters, mean and fluctuating velocity components only, since these have been investigated extensively in experiments and would be expected to be rather consistent between various simulations. However, based on these results, the concept of a 'numerical experiment' (see e.g. Kasagi & Shikazono 1995) is clearly supported, indicating that even DNS data should be the subject of the same scrutiny as experimental data.

In the following, statistically two-dimensional boundary layers are considered which are evolving in the streamwise (x) direction; the wall-normal direction is denoted by y. The notation is based on the Reynolds decomposition of an instantaneous quantity into a spanwise and temporal average U and a respective fluctuating part u. Based on the two-dimensional mean profile $U(x, y)$, the shear stress at the wall is obtained as $\tau_w(x) = \mu(\mathrm{d}U/\mathrm{d}y)|_{y=0}$. The relevant velocity and length scales close to the wall are then given by $U_\tau = \sqrt{\tau_w/\rho}$ and $\ell_\star = \nu/U_\tau$. Quantities in wall scaling are thus written as, e.g. $U^+ = U/U_\tau$ and $y^+ = y/\ell_\star$. The outer scales are given by the free-stream velocity $U_\infty = U(y \to \infty)$ and the 99 % boundary-layer thickness δ_{99}.

2. Selection of data and new simulation

Compared to e.g. turbulent channel flow, the number of (numerical) data bases for spatially evolving TBLs at medium to high Reynolds numbers ($Re_\theta > 650$) is small. In the following, results from Spalart (1988), Komminaho & Skote (2002), Khujadze & Oberlack (2004, 2007), Schlatter *et al.* (2009*a*, *b*), Ferrante & Elghobashi (2005), Simens *et al.* (2009) and Wu & Moin (2009) have been considered. A summary of the key characteristics of these data bases is given in table 1 together with their

Reference	Re_θ	Method	Symbol
Spalart (1988)	300, 600 and 1410	Spectral Spatio-temporal	+
Komminaho & Skote (2002)	383–716	Spectral Tripping at $Re_\theta \approx 200$ Domain up to $Re_\theta \approx 750$	●
Khujadze & Oberlack (2004, 2007)	489–2807	Spectral Tripping close to resp. inflow Domain length $\Delta Re_\theta \approx 500$	□
Ferrante & Elghobashi (2005)	2900	Finite differences Rescaling and recycling Domain $Re_\theta = 2340$–2900	×
Simens *et al.* (2009)	1000, 1550 and 1968	Finite-difference/spectral Rescaling and recycling Domain $Re_\theta = 620$–2140	■
Schlatter *et al.* (2009*a*, *b*)	677–4271	Spectral Tripping at $Re_\theta = 180$, single Domain up to $Re_\theta \approx 4300$	○
Wu & Moin (2009)	800, 900	Finite difference Free-stream disturbances Laminar inflow at $Re_\theta = 80$	*

TABLE 1. List of utilized DNS data bases, the Reynolds numbers and the key characteristics of the applied simulation method. If more than three profiles have been used from a given reference, only the range of Reynolds numbers is given.

parameter range. For all data bases, only the region considered 'fully turbulent' by the original authors has been included here; for instance, Wu & Moin (2009) state for their simulation that 'transition is complete by $Re_\theta = 750$'. Most of the data selected here employed experimental results (e.g. those of Erm & Joubert 1991; Österlund 1999; Örlü 2009, among others) to compare and validate their simulations.

To complement the existing data bases available in the literature, a new simulation has recently been performed at the Royal Institute of Technology (KTH), Stockholm (Schlatter *et al.* 2009*a*). This new DNS is based on the same fully spectral numerical method as used by Schlatter *et al.* (2009*b*), and uses the same computational domain as Schlatter *et al.* (2010). An extended range of $Re_\theta = 180$–4300 is then simulated in a domain that is at least three times wider and higher than the maximum δ_{99}. A total of $8192 \times 513 \times 768$ spectral modes are employed, yielding a resolution in physical space of $\Delta x^+ \approx 9$ and $\Delta z^+ \approx 4$. This resolution is comparable to high-Re channel-flow simulations such as e.g. Hoyas & Jiménez (2006) and slightly higher than in the previous boundary-layer simulation (Schlatter *et al.* 2009*b*). This simulation includes, to the authors' knowledge, the largest Reynolds-number range as well as the highest simulated Reynolds number for DNS of TBL flows.

With the notable exception of Spalart (1988), all the simulations presented here consider truly spatially evolving boundary layers. Such a simulation approach is generally considered the most natural, and thus most accurate, however, it requires special means to introduce turbulence in the flow. Different methods have been followed here, including recycling and rescaling (introduced by Lund, Wu & Squires 1998) of the turbulence from a more downstream position (Ferrante & Elghobashi 2005; Simens *et al.* 2009), inducing laminar-turbulent transition via free-stream disturbances (Wu & Moin 2009), and triggering laminar-turbulent transition at lower

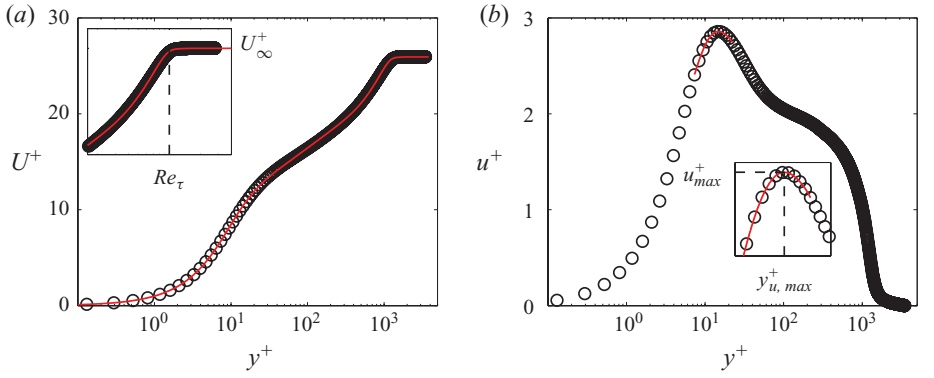

FIGURE 1. DNS data by Schlatter *et al.* (2009*a*) for $Re_\theta = 4064$. (*a*) Inner-scaled mean streamwise velocity profile. The insert enlarges the wake part and illustrates the quality of the fit as well as the computed values for $Re_\tau = \delta^+_{99}$ and U^+_∞. (*b*) Inner-scaled streamwise turbulence intensity profile. The insert enlarges the vicinity of the near-wall peak and illustrates the quality of the fourth-order polynomial fit as well as the computed peak value and position.

(Komminaho & Skote 2002; Schlatter *et al.* 2009*a*, *b*) and at higher Reynolds numbers (Khujadze & Oberlack 2004). Apart from different numerical discretization schemes and resolutions, the simulations outlined in table 1 feature largely varying domain lengths and inflow Reynolds numbers. In this regard, it is interesting to recall the recent finding by Simens *et al.* (2009) saying that in their simulation, the boundary layer needed to develop for at least 300 initial momentum thicknesses in order to forget the effect of the artificial inflow. In the comparison discussed in this study, the longest domains are employed by Simens *et al.* (2009) and Schlatter *et al.* (2009*a*,*b*); in the latter case, the computational domain extends over nearly one order of magnitude in Re_θ. For further details of the exact numerical methods and specific simulation parameters, it is referred to the original publications.

In some figures, the well-known channel-flow data from Iwamoto, Suzuki & Kasagi (2002), Abe, Kawamura & Matsuo (2004), del Álamo & Jiménez (2003), del Álamo *et al.* (2004), Hoyas & Jiménez (2006), Kawamura, Abe & Matsuo (1999) and Tsukahara *et al.* (2005) have been utilized for comparisons.

3. Organization of results

When comparing results from different sources, it is important to employ consistent definitions for the various measured quantities. Otherwise, not only quantitative changes could be obscured, but also different qualitative trends might be obtained based on slightly incompatible definitions. For the data presented in this paper, this has been found to be particularly the case for the shape factor, defined as the ratio of displacement and momentum thickness, $H_{12} = \delta^*/\theta$. Owing to different conditions in the free stream (e.g. the slope of U_∞), the availability of data points outside the boundary layer, and the total height of the computational domain, varying values for H_{12} are obtained depending on the exact definition. Thus, in an effort to ease comparability, certain quantities have been recomputed in a consistent manner for all data sets by means of a composite mean streamwise velocity profile, i.e. the one proposed by Nickels (2004) (see figure 1*a*). The choice for this particular composite profile for the extraction of the free-stream velocity U^+_∞ and the boundary-layer thickness (or Kármán number) δ^+_{99} is due to its excellent description of the wake part

of the velocity profile even at the low Reynolds numbers considered here. Based on these parameters, new values for the shape factor and the Reynolds numbers based on displacement and momentum thickness can be computed by evaluating the integrals from the wall up to δ_{99}^+,

$$H_{12} = \frac{Re_{\delta^*}}{Re_\theta} = \frac{\displaystyle\int_0^{\delta_{99}^+} \left(1 - \frac{U^+}{U_\infty^+}\right) \mathrm{d}y^+}{\displaystyle\int_0^{\delta_{99}^+} \frac{U^+}{U_\infty^+} \left(1 - \frac{U^+}{U_\infty^+}\right) \mathrm{d}y^+}. \tag{3.1}$$

It was, however, decided to keep Re_θ as provided by the original authors in order to ease identification of the individual measurement points. The re-evaluated values would in most cases yield slightly smaller values, but the qualitative trends would be unaffected. In addition, also the friction coefficient c_f, and thus the viscous scaling could be obtained from the composite fit. However, it turned out that c_f was only changed by about 0.1 % compared to employing the value of U^+ at the upper domain boundary. Therefore, we stick to the latter definition here, which is also the convention that most authors have used to define their viscous scaling.

To evaluate the peak values and the respective positions for the various components of the Reynolds stress tensor, an interpolation based on a fourth-order polynomial fit to the data in the vicinity of the maximum has been used, as illustrated in figure 1(*b*). In this way, the results become independent of the exact point distribution around the maxima.

The value for the fluctuating wall shear stress $\tau_{w,rms}^+$ has been obtained through the limiting behaviour of the local streamwise turbulence intensity (Alfredsson *et al.* 1988):

$$\tau_{w,rms}^+ = \lim_{y^+ \to 0} \frac{u^+}{U^+}. \tag{3.2}$$

For the simulation with the coarsest grid in the near-wall region (Ferrante & Elghobashi 2005), the closest point to the wall is at $y^+ = 0.6$, all other simulations provided data points < 0.3 wall units, thus ensuring an accurate approximation of $\tau_{w,rms}^+$ in all cases.

When channel-flow results are shown for comparison, Re_τ is used on the abscissa, although Re_{δ^*} or Re_θ would be more appropriate for boundary-layer flows. The length scale in Re_τ is then given by either the channel half-height h or the boundary-layer thickness δ_{99}, respectively.

4. Results and discussion

4.1. *Shape factor and skin friction*

The shape factor, H_{12}, gives a direct quantitative assessment of the mean streamwisevelocity profile independent of the skin friction (i.e. wall-normal derivatives). The values obtained for all simulations listed in table 1 are shown in figure 2(*a*). The solid and dashed lines depict the integration of the composite profile by Chauhan *et al.* (2009) and its 1 % tolerance limits. Since this composite profile is based on medium-to-high Reynolds-number ZPG TBL experiments, it should serve here mainly as an indicator for the scatter in the data. Nevertheless, it is worth noting that the data by Schlatter *et al.* (2009*b*) is in very good agreement with the composite profile, as are the ones by Simens *et al.* (2009) and Komminaho & Skote (2002). On

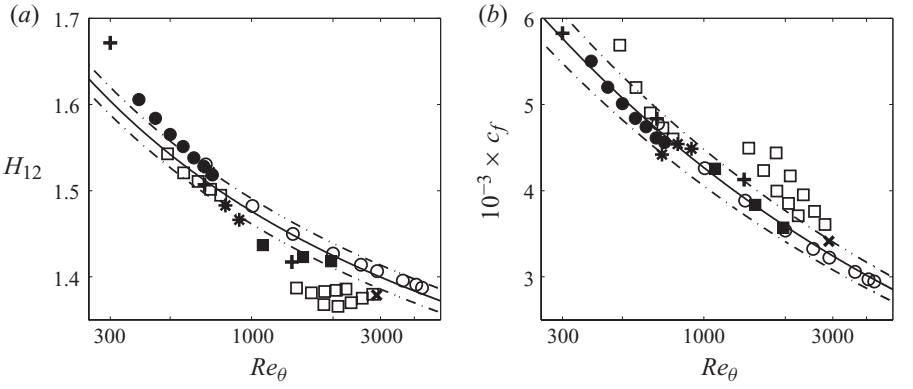

FIGURE 2. (*a*) Shape factor, H_{12}, as function of Reynolds number. Solid line represents the integration of composite profile (Chauhan *et al.* 2009) and the dash-dotted lines indicate a 1 % tolerance. (*b*) Skin-friction coefficient, c_f, as function of Reynolds number. Solid line represents the correlation by Smits, Matheson & Joubert (1983) and dash-dotted lines indicate a 5 % tolerance.

the other hand, the shape factors from Spalart (1988) show a different Re trend, and the ones by Khujadze & Oberlack (2004) even increase with increasing Re for some cases.

The skin-friction coefficient, c_f, for the same set of data is depicted in figure 2(*b*) together with the simple empirical correlation based on the 1/7-power law of the form $c_f = 0.024 Re_\theta^{-1/4}$ (Smits *et al.* 1983) and its 5 % tolerance limits. Interestingly, the scatter in the DNS data is as large as in similar experimental compilations, where most of the skin-friction values have been extracted by indirect methods. In addition, it is not only the actual values of c_f that differ, but also inconsistent trends with respect to Re_θ: this could be an indication that some of the simulated boundary layers were still developing and have not yet reached their final turbulent equilibrium state.

In an effort to compare internal and external flows, all available TBL data have been employed to obtain a functional relation for Re_τ in terms of Re_θ, although Re_θ and Re_δ^* are more meaningful for boundary layers. The linear behaviour in figure 3(*a*) suggests a power-law relation, and indeed $Re_\tau = 1.13 \times Re_\theta^{0.843}$ provides a good fit to the data and can be used to convert between the two Reynolds numbers.

To further quantify the turbulence in the near-wall region, the fluctuation magnitude of the wall-shear stress, $\tau_{w,rms}^+$ is depicted together with the values for channel flows in figure 3(*b*). As predicted by Alfredsson *et al.* (1988), a value around 0.4 is found in all cases, with a slight increase with Reynolds number: utilizing the data by Komminaho & Skote (2002), Simens *et al.* (2009) and Schlatter *et al.* (2009*a*), a relation $\tau_{w,rms}^+ = 0.298 + 0.018 \ln Re_\tau$ is obtained (cf. a similar relation in Schlatter *et al.* 2010). The trend for TBL flows compares favourably to the one for channel flows at higher Re. The deviations for the lower Reynolds numbers might be due to the effect of pressure gradient, which is not negligible for channel flows at such low Reynolds numbers. The simulation by Wu & Moin (2009) gives the highest prediction for $\tau_{w,rms}^+$, which is not supported by the other data, neither in channel nor in boundary-layer geometry. The reason for this behaviour is not known, but might be related to the relative proximity of the measurement points to the laminar-turbulent changeover. It thus appears that in particular $\tau_{w,rms}^+$ can be used as a useful

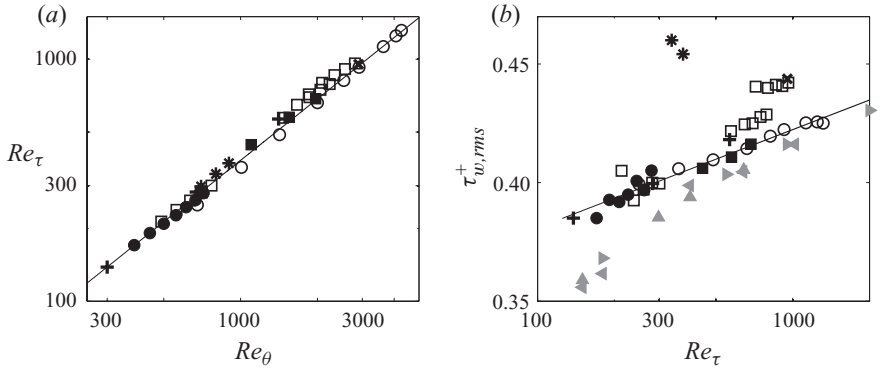

FIGURE 3. (*a*) Relation between Reynolds numbers Re_θ and $Re_\tau = \delta^+_{99}$. Solid line represents best fit to all data points, viz. $Re_\tau = 1.13 \times Re_\theta^{0.843}$. (*b*) Fluctuating wall-shear stress, $\tau^+_{w,rms}$, as function of the friction Reynolds number. Best fit to data by Komminaho & Skote (2002), Simens *et al.* (2009), Schlatter *et al.* (2009*a*): $\tau^+_{w,rms} = 0.298 + 0.018 \ln Re_\tau$. Channel-flow DNS data (filled grey symbols): (◄) (Kawamura *et al.* 1999; Abe *et al.* 2004; Tsukahara *et al.* 2005), (▲) (Iwamoto *et al.* 2002) and (►) (del Álamo & Jiménez 2003; del Álamo *et al.* 2004; Hoyas & Jiménez 2006).

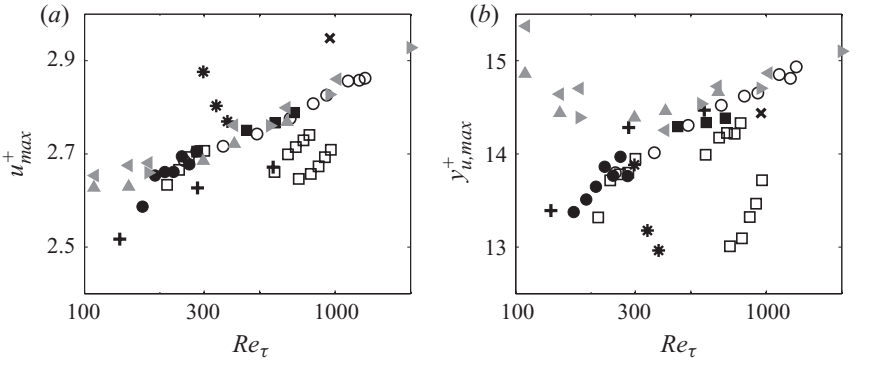

FIGURE 4. Near-wall behaviour of inner-scaled streamwise velocity fluctuation. (*a*) Value and (*b*) wall-normal position of maximum. Corresponding channel-flow DNS values are depicted in filled grey symbols (see figure 3*b* for references).

measure to judge whether the near-wall turbulence of a given flow has reached its final turbulent state.

4.2. *Streamwise velocity profiles*

Having displayed considerable differences in the shape factor and skin friction, it is now interesting to consider profiles of the streamwise velocity in more detail. In a first step, the fluctuations u in a region close to the wall are considered; naturally, for all simulations profiles similar to the one shown in figure 1(*b*) are obtained. The maximum values for the different simulations and the respective wall-normal position are reported in figure 4. Again, a fairly large spread of the data with a variation of up to 10 % at a fixed Re_τ can be observed. Note that the spanwise resolution of a simulation has a direct influence on the fluctuation maximum, reducing u^+_{max} by about 1 % going from $\Delta z^+ \approx 5$ to $\Delta z^+ \approx 10$. However, the bulk of the data seems to be in reasonable agreement with corresponding channel data, in particular for the fluctuation maximum u^+_{max}, but also for its position, provided Re_τ is large enough.

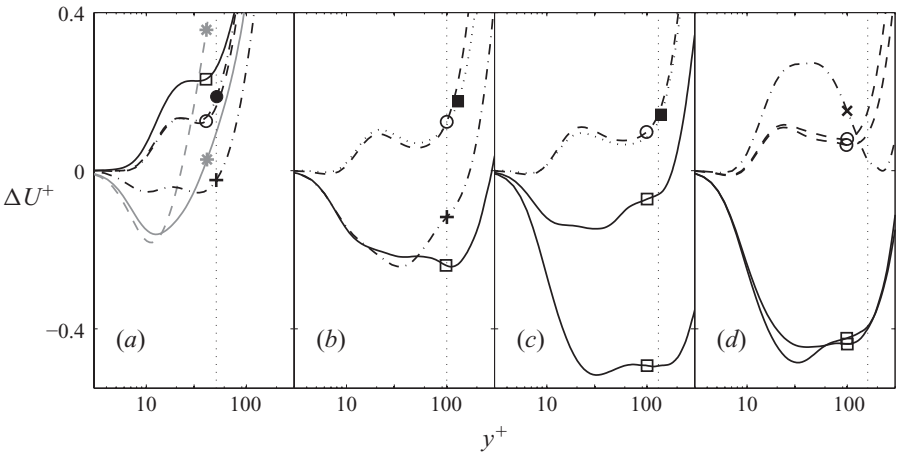

FIGURE 5. Deviation of mean-velocity profile from the modified Musker profile in the inner region clustered in four Reynolds-number regions. (*a*) $Re_\theta = 666$ (Komminaho & Skote 2002), 670 (Spalart 1988), 677 (Schlatter *et al.* 2009*a*), 705 (Khujadze & Oberlack 2004), 700 and 800 (Wu & Moin 2009). (*b*) $Re_\theta = 1410$ (Spalart 1988), 1421 (Schlatter *et al.* 2009*a*), 1469 (Khujadze & Oberlack 2004), 1551 (Simens *et al.* 2009). (*c*) $Re_\theta = 1968$ (Simens *et al.* 2009), 2000 (Schlatter *et al.* 2009*a*), 2055 and 2087 (Khujadze & Oberlack 2004). (*d*) $Re_\theta = 2536$ and 2911 (Schlatter *et al.* 2009*a*), 2568 and 2807 (Khujadze & Oberlack 2004), 2900 (Ferrante & Elghobashi 2005). Dashed vertical lines indicate the wall-normal boundary of the overlap region for the lowest Reynolds number, i.e. $y^+/Re_\tau = 0.2$.

Similar observations can also be made for the maxima in the other components of the stress tensor, and are thus not shown here.

The mean profiles in the inner region are usually considered quite comparable between various simulations. However, minor differences have been shown to exist also for different channel-flow simulations at the same Re_τ (Örlü 2009). To highlight such a behaviour in boundary layers, we consider in figure 5 the difference between the simulated profiles and a composite velocity-profile description, i.e. $\Delta U^+ = U^+ - U^+_{CP}$. Here, the composite profile by Chauhan *et al.* (2009) has been employed rather than the one by Nickels (2004), since it was found that the former description provides the closest fit to quality experiments and DNS data within the sublayer (Örlü 2009). In order to minimize Reynolds-number effects, the plots are clustered around four narrow Reynolds-number ranges centred around $Re_\theta = 670$, 1410, 2000 and 2900. Furthermore, the wall-normal boundary of the overlap region, chosen as $0.2\,\delta^+_{99}$, has been included in the figure to illustrate from where on differences can be attributed to the wake region containing weak-Reynolds-number effects even within the narrow-Reynolds-number range. It can be seen that the simulation data by Komminaho & Skote (2002), Simens *et al.* (2009) and Schlatter *et al.* (2009*a*) are essentially showing the same quantitative and qualitative behaviour irrespective of the Reynolds number, whereas the other profiles feature clear differences even within the buffer region ($y^+ \approx 20$). These differences should particularly be considered in the light of the common utilization of near-wall DNS data to extract the skin friction, and to correct the absolute wall distance by fitting experimental data.

4.3. *Discussion*

The results presented in this section clearly show that different simulations, all pertaining to the same canonical flow case, give surprisingly inconsistent predictions

for quantities as basic as the friction coefficient, shape factor and fluctuation maxima. Note that the presented quantities should be considered as a number of examples, not an exhaustive list of all possible discrepancies between the simulations. All the DNS data included here were obtained based on reliable numerical methods with sufficiently high resolutions such that the discrepancies cannot be solely attributed to poor numerics. Thus, the differences must come from different decisions in the (numerical) set-up of a simulation, which can be categorized roughly as follows: (i) inflow Reynolds number and turbulence generation, (ii) sufficient settling length to reach final turbulent state, and (iii) box dimensions and boundary conditions (e.g. pressure gradients). In that regard, it is not surprising that the simulations with the largest domains (Simens *et al.* 2009; Schlatter *et al.* 2009*a*) are also the ones that appear to yield results closest to each other and to established relations. On the other hand, short boxes, measurement points close to transition, strong forcings towards turbulence at high-Re number are all factors that might lead to inaccurate turbulence conditions. Note that very similar considerations must be taken into account also for experimental studies (see also the discussion by Erm & Joubert 1991): choice of tripping device, sufficient settling length after the tripping, stagnation-line settings, possible blockage in the wind tunnel and pressure-gradients due to tunnel walls. For instance, an auxiliary simulation based on LES similar to Schlatter *et al.* (2010) with inflow and tripping located at high $Re_\theta \approx 2000$ yields comparable results to Khujadze & Oberlack (2007): the necessary inflow length for developed turbulence at higher Re is longer, which is evidenced by e.g. an increasing shape factor (see figure 2*a*).

It is thus the purpose of the present paper to clearly highlight the fact that even for moderately complex flow cases such as a canonical spatially evolving TBL, the proper set-up of a simulation is of crucial importance to obtain accurate and reliable simulation results. Very much in the same way as a physical experiment in a wind tunnel, a simulation has to be considered a numerical experiment governed by the chosen simulation set-up such as boundary conditions, box dimensions and resolution (see among others Kasagi & Shikazono 1995). It is only when verifying all aspects of a simulation, e.g. by critically comparing to other simulations, experiments, theories, best-practise guidelines, refinement studies, etc. that DNS data can be taken as reference data. Therefore, any DNS should be subjected to the same scrutiny as experimental data.

However, as also shown in the present contribution, if simulations are set up with sufficient care they can certainly lead to very robust and accurate predictions.

5. Conclusions

The canonical TBL under ZPG has been a research topic for a number of decades; still fundamental open questions exist related to, e.g. scaling and shape of the mean and fluctuation profiles. In the experimental community, it has been realized that the exact documentation of an experiment is crucial to provide accurate, reliable and reproducible results; both related to the physical set-up of the experiment (tunnel geometry, tripping, etc.) and the applied measurement technique (temporal and spatial resolution, correction methods for Pitot tubes, etc.).

On the other hand, a number of new DNS of such canonical TBLs has been performed in recent years, complementing and extending the results obtained by the early simulation of Spalart (1988). DNS have the clear advantage that, among others, all the case-specific parameters (inflow, boundary conditions, disturbances, etc.) can be set accurately, and no random measurement error corrupts the obtained data.

Thus, DNS data are usually considered to be more accurate and more reliable than corresponding experiments. This is certainly true in cases when boundary conditions can be specified unambiguously as for instance in turbulent channel flow.

It is the goal of this study to investigate the similarities and differences present in a number of recent DNS data bases, all of which simulating the same generic-flow case, i.e. a boundary layer with ZPG. These considered data sets also include a recent DNS with the extended range of Reynolds numbers $Re_\theta = 500$–4300. The resulting comparison shows surprisingly large differences not only in both basic integral quantities such as the friction coefficient c_f or the shape factor H_{12}, but also in their predictions of mean and fluctuation profiles. It is thus shown that the numerical simulation of TBLs is, mainly due to the spatial development of the flow, very sensitive towards, e.g. proper inflow condition, settling length and appropriate box dimensions. Thus, a DNS has to be considered a numerical experiment and should be the subject of the same scrutiny as experimental data. However, if a DNS is set up with the necessary care, it can provide a faithful tool to predict even such notoriously difficult flow cases with great accuracy. This is clearly shown as the simulations which include the longest streamwise domains (largest span of Re_θ in a single domain) appear also to provide the most reliable predictions for various turbulence quantities.

The original authors of the various data bases used in this study are gratefully acknowledged for sharing their simulation data. Computer time was provided by Swedish National Infrastructure for Computing (SNIC) with a generous grant by the Knut and Alice Wallenberg (KAW) Foundation. Some of the simulations were run at the Centre for Parallel Computers (PDC), Royal Institute of Technology (KTH) and the National Supercomputer Centre (NSC), Linköping University in Sweden.

REFERENCES

Abe, H., Kawamura, H. & Matsuo, Y. 2004 Surface heat-flux fluctuations in a turbulent channel flow up to $Re_\tau = 1020$ with $Pr = 0.025$ and 0.71. *Intl J. Heat Fluid Flow* **25**, 404–419.

del Álamo, J. & Jiménez, J. 2003 Spectra of the very large anisotropic scales in turbulent channels. *Phys. Fluids* **15**, L41–L44.

del Álamo, J., Jiménez, J., Zandonade, P. & Moser, R. D. 2004 Scaling of the energy spectra of turbulent channels. *J. Fluid Mech.* **500**, 135–144.

Alfredsson, P. H., Johansson, A. V., Haritonidis, J. H. & Eckelmann, H. 1988 The fluctuating wall-shear stress and the velocity field in the viscous sublayer. *Phys. Fluids* **31**, 1026–1033.

Buschmann, M. H., Indinger, T. & Gad-el-Hak, M. 2009 Near-wall behaviour of turbulent wall-bounded flows. *Intl J. Heat Fluid Flow* **30**, 993–1006.

Chauhan, K. A., Monkewitz, P. A. & Nagib, H. M. 2009 Criteria for assessing experiments in zero pressure gradient boundary layers. *Fluid Dyn. Res.* **41**, 021404.

Erm, L. P. & Joubert, P. 1991 Low-Reynolds-number turbulent boundary layers. *J. Fluid Mech.* **230**, 1–44.

Fernholz, H. H. & Finley, P. 1996 The incompressible zero-pressure-gradient turbulent boundary layer: an assessment of the data. *Prog. Aerosp. Sci* **32**, 245–311.

Ferrante, A. & Elghobashi, S. E. 2005 Reynolds number effect on drag reduction in a microbubble-laden spatially developing turbulent boundary layer. *J. Fluid Mech.* **543**, 93–106.

Hoyas, S. & Jiménez, J. 2006 Scaling of the velocity fluctuations in turbulent channels up to $Re_\tau = 2003$. *Phys. Fluids* **18**, 011702.

Iwamoto, K., Suzuki, Y. & Kasagi, N. 2002 Reynolds number effect on wall turbulence: toward effective feedback control. *Intl J. Heat Fluid Flow* **23**, 678–689.

Kasagi, N. & Shikazono, N. 1995 Contribution of direct numerical simulation to understanding and modelling turbulent transport. *Proc. R. Soc. Lond.* A **451**, 257–292.

Kawamura, H., Abe, H. & Matsuo, Y. 1999 DNS of turbulent heat transfer in channel flow with respect to Reynolds and Prandtl number effects. *Intl J. Heat Fluid Flow* **20**, 196–207.

Khujadze, G. & Oberlack, M. 2004 DNS and scaling laws from new symmetry groups of ZPG turbulent boundary layer flow. *Theor. Comput. Fluid Dyn.* **18**, 391–411.

Khujadze, G. & Oberlack, M. 2007 New scaling laws in ZPG turbulent boundary layer flow. In *Proceedingsof the Fifth International Symposium on Turbulence and Shear Flow Phenomena*, München, Germany, pp. 443–448.

Komminaho, J. & Skote, M. 2002 Reynolds stress budgets in Couette and boundary layer flows. *Flow Turbul. Combust.* **68**, 167–192.

Lund, T. S., Wu, X. & Squires, K. D. 1998 Generation of turbulent inflow data for spatially-developing boundary layer simulations. *J. Comput. Phys.* **140**, 233–258.

Monkewitz, P. A., Chauhan, K. A. & Nagib, H. M. 2008 Comparison of mean flow similarity laws in zero pressure gradient turbulent boundary layers. *Phys. Fluids* **20**, 105102.

Nickels, T. B. 2004 Inner scaling for wall-bounded flows subject to large pressure gradients. *J. Fluid Mech.* **521**, 217–239.

Örlü, R. 2009 Experimental studies in jet flows and zero pressure-gradient turbulent boundary layers. PhD thesis, Royal Institute of Technology, Stockholm, Sweden.

Österlund, J. M. 1999 Experimental studies of zero pressure-gradient turbulent boundary layer flow. PhD thesis, Royal Institute of Technology, Stockholm, Sweden.

Schlatter, P., Li, Q., Brethouwer, G., Johansson, A. V. & Henningson, D. S. 2009*a* High-Reynolds number turbulent boundary layers studied by numerical simulation. *Bull. Am. Phys. Soc.* **54**, 59.

Schlatter, P., Örlü, R., Li, Q., Brethouwer, G., Fransson, J. H. M., Johansson, A. V., Alfredsson, P. H. & Henningson, D. S. 2009*b* Turbulent boundary layers up to $Re_\theta = 2500$ studied through simulation and experiment. *Phys. Fluids* **21**, 051702.

Schlatter, P., Li, Q., Brethouwer, G., Johansson, A. V. & Henningson, D. S. 2010 Simulations of spatially evolving turbulent boundary layers up to $Re_\theta = 4300$. *Intl J. Heat Fluid Flow* **31**, 251–261.

Simens, M. P., Jiménez, J., Hoyas, S. & Mizuno, Y. 2009 A high-resolution code for turbulent boundary layers. *J. Comput. Phys.* **228**, 4218–4231.

Smits, A. J., Matheson, N. & Joubert, P. N. 1983 Low-Reynolds-number turbulent boundary layers in zero and favourable pressure gradients. *J. Ship Res.* **27**, 147–157.

Spalart, P. 1988 Direct simulation of a turbulent boundary layer up to $R_\theta = 1410$. *J. Fluid Mech.* **187**, 61–98.

Tsukahara, T., Seki, Y., Kawamura, H. & Tochio, D. 2005 DNS of turbulent channel flow at very low Reynolds numbers. In *Proceedings of the Fourth International Symposium on Turbulence and Shear Flow Phenomena*, Williamsburg, VA, pp. 935–940.

Wu, X. & Moin, P. 2009 Direct numerical simulation of turbulence in a nominally zero-pressure-gradient flat-plate boundary layer. *J. Fluid Mech.* **630**, 5–41.